EFFECTS OF PROCESS PARAMETERS AND HEAT TREATMENT ON THE MICROSTRUCTURE AND MECHANICAL PROPERTIES OF SELECTIVE LASER MELTED INCONEL 718

Wenpu Huang, Zemin Wang, Jingjing Yang, Huihui Yang, and Xiaoyan Zeng

Wuhan National Laboratory for Optoelectronics
Huazhong University of Science and Technology, Wuhan, PR China

Abstract

In this study, Inconel 718 superalloy was fabricated by selective laser melting (SLM) and solution treated at 980-1230 ℃ subsequently. The process window was firstly set up based on the density of the samples. Samples were fabricated using various parameters within the process window to investigate the effects of process parameters on microstructure and mechanical properties. The average dendrite arm spacing and the volume fraction of Laves phase raise along with the increasing energy input. However, no distinct difference of tensile properties was found under parameters in the process window. Interdendritic Laves phase decreases with the solution temperature, while the grain size has the opposite trend. Finally, the solution temperature was fixed at 1080 ℃ to dissolve Laves phases and obtain fine grains. After solution + aging heat treatment, the tensile strengths and ductility all exceed the wrought Inconel 718.

Keywords: Selective laser melting; Process parameters; Heat treatment; Microstructure; Mechanical properties

Introduction

Selective laser melting (SLM) is a rapidly developing advanced manufacturing technique which melts the metal powders with the laser beam to build parts layer by layer directly from CAD model [1, 2]. Compared with conventional manufacturing processes, SLM offers its unique advantages, such as high dimension accuracy and geometrical complexity, material saving and reduction of product cycles [3, 4]. Therefore, the technique has gained widespread interest recently.

Inconel 718 (IN718) superalloy is widely applied in aerospace and energy industries due to its excellent strength at elevated temperatures, good corrosion resistance and favorable weldability [5-7]. Extensive work has been conducted on selective laser melted IN718 at present [1, 2, 4, 8-15]. The microstructure, mechanical properties, heat treatment and residual stress of SLMed IN718 has been studied. However, most of research adopted the optimal process parameters to produce the samples aimed at the minimisation of porosity, and only limited work has focused on the correlation between process parameters, microstructure and properties [11]. Therefore, in this work, effects of process parameters on microstructure and mechanical properties of SLMed IN718 have been studied and the effects of heat treatment were also evaluated.

Materials and Methods

Gas atomized IN718 powders with an average diameter of 31 μm were chosen as the starting materials in this work and the chemical composition is shown in Table 1. All the samples were fabricated by a self-developed SLM machine equipped with an IPG YLR-500 fiber laser (maximum output power of 500 W) .

Table1 Chemical composition of IN718 powder

Element	Ni	Cr	Fe	Nb	Mo	Ti	Al	Co	Mn	C
wt.%	Balance	18.46	18.45	5.1	3.04	0.9	0.66	0.16	0.17	0.054

Two kinds of samples were produced: cubic samples ($10\times10\times8$ mm^3) and tensile test samples. Cubic samples were fabricated using various process parameters shown in Table 2 to optimize the parameters based on the relative density of the samples. Tensile test samples designed according to ISO 6892-1-2009 were built horizontally using the optimal parameters.

Table 2 SLM process parameters applied in this study.

Process parameter	Value
Laser power P (W)	150-500
Scanning velocity v (mm/s)	400-1400
Hatch spacing h (mm)	0.08, 0.10, 0.12
Layer thickness t (μm)	20, 40, 60

In order to investigate the effects of heat treatment on microstructure and mechanical properties, the as-fabricated samples were solution treated at different temperatures (980-1230 ℃) for 1 h followed by air cooling and conventional double aging treatment (720 °C/8 h + 620 °C/8 h, AC) was adopted. All the heat treatments were carried out using a KSL-1400X-A2 muffle furnace with a heating rate of 10 ºC/min.

The relative density of the samples were measured using the Image-Pro Plus 6.0 software. For microstructure research, the samples were etched by a solvent consisting of 30 ml HCl + 10 ml HNO_3 after grinding and mechanical polishing. The microstructure was characterized using a Nikon Epiphot-300 optical microscope (OM), a FEI Sirion 200 scanning electron microscopy (SEM) and a FEI Quanta 200 scanning electron microscopy. Tensile test were conducted at room temperature using a Shimadzu AG-100 kN tester.

Results and discussions

Effects of process parameters

A series of cubic samples were fabricated using the process parameters shown in Table 2 and the relative density was measured. Based on the results, certain process parameters which guarantee the samples with relative density > 99.9% were selected for further study as shown in Table 3. Sample P1, P2 and P3 only differ in layer thickness and hence they were compared to reveal the effects of layer thickness. Similarly, Sample P3, P7 and P9 were compared to reveal the effects of laser power, Sample P4, P5 and P6 were compared to reveal the effects of scanning velocity, Sample P6, P7 and P8 were compared to reveal the effects of hatch spacing.

Table 3 The selected process parameters which guarantee the samples with relative density > 99.9%.

Sample	Layer thickness t (μm)	Laser power P (W)	Scanning velocity v (mm/s)	Hatch spacing h (mm)
P1	20	300	1000	0.10
P2	40	300	1000	0.10
P3	60	300	1000	0.10
P4	60	400	600	0.08
P5	60	400	800	0.08
P6	60	400	1000	0.08
P7	60	400	1000	0.10
P8	60	400	1000	0.12
P9	60	500	1000	0.10

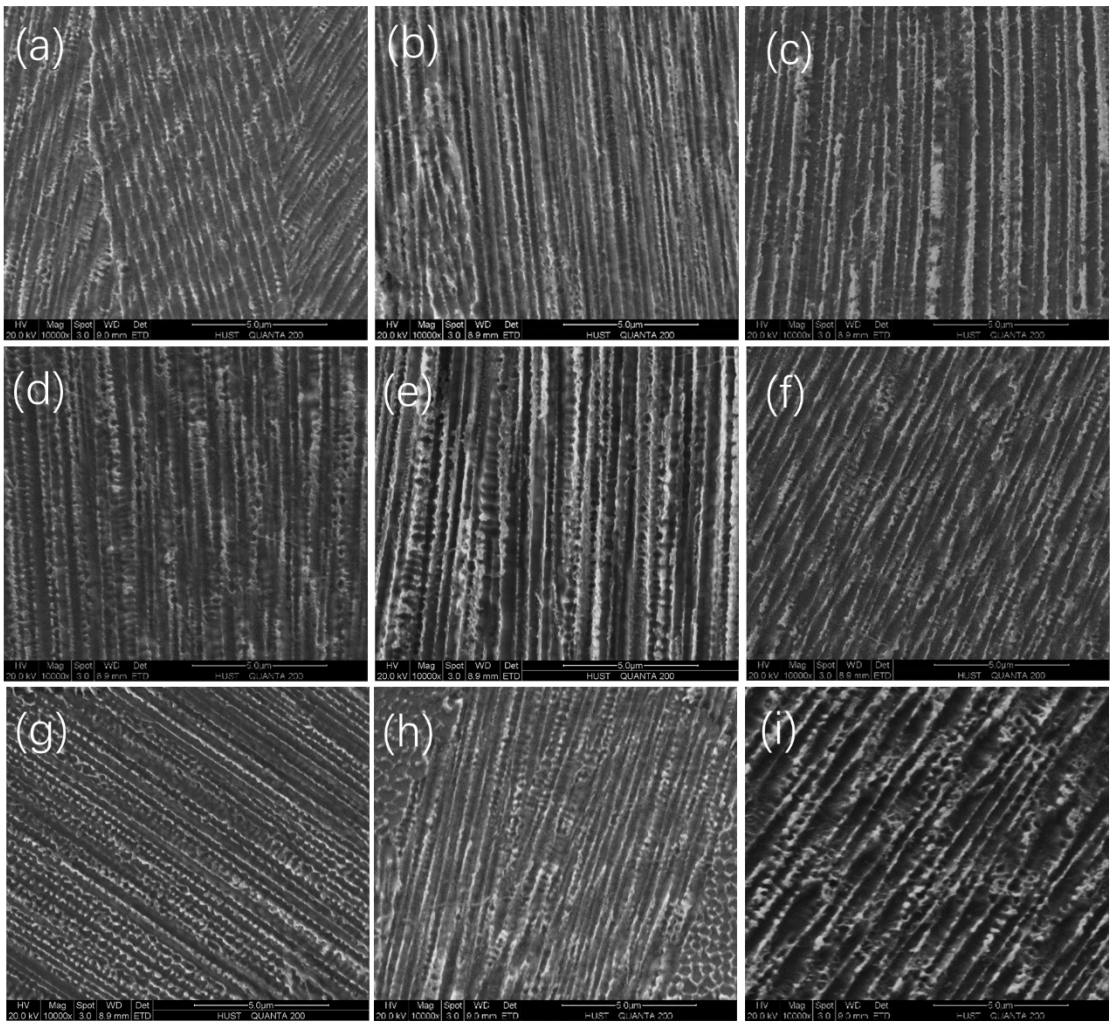

Fig. 1. Microstructures of samples fabricated with different process parameters : (a) P1; (b) P2; (c) P3; (d) P4; (e) P5; (f) P6 (g) P7; (h) P8; (i) P9.

Fig. 1 presents the microstructures of IN718 samples produced with different process parameters. It shows that due to the high cooling rates during SLM process, the as-fabricated samples are characterized with fine cellular dendrites with Laves phase precipitating in the interdendritic regions. The formation of Laves phase results from the segregation of alloy elements such as Nb and Mo [16]. In addition, the presence of the phase will weaken the precipitation of γ′ and γ″ [15]. In order to investigate the effects of process parameters on the microstructure, the average dendrite arm spacing and the volume fraction of Laves phase were measured. The binary processing of SEM images were conducted to facilitate the measurements of the volume fraction as shown in Fig. 2. The black regions are γ matrix, while the white regions are Laves phase. The statistic results are shown in Fig.3. As can be seen, the average dendrite arm spacing and the volume fraction of Laves phase raise along with increasing laser power and decreasing scanning velocity and hatch spacing, while the effect of hatch spacing on the average dendrite arm spacing is not distinct. The increasing energy input results in lower cooling rate, which leads to the increase of the average dendrite arm spacing. In addition, Nb elements have more time to diffuse due to the lower cooing rate [13]. As a result, it will contribute to the formation of Laves phase.

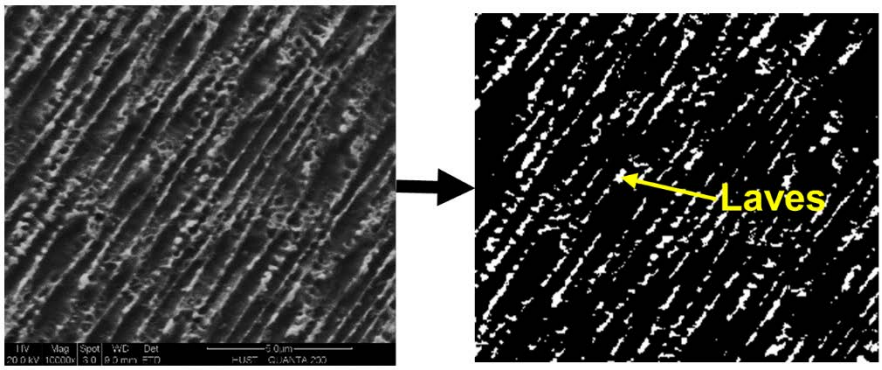

Fig. 2. Sketch of binary image processing

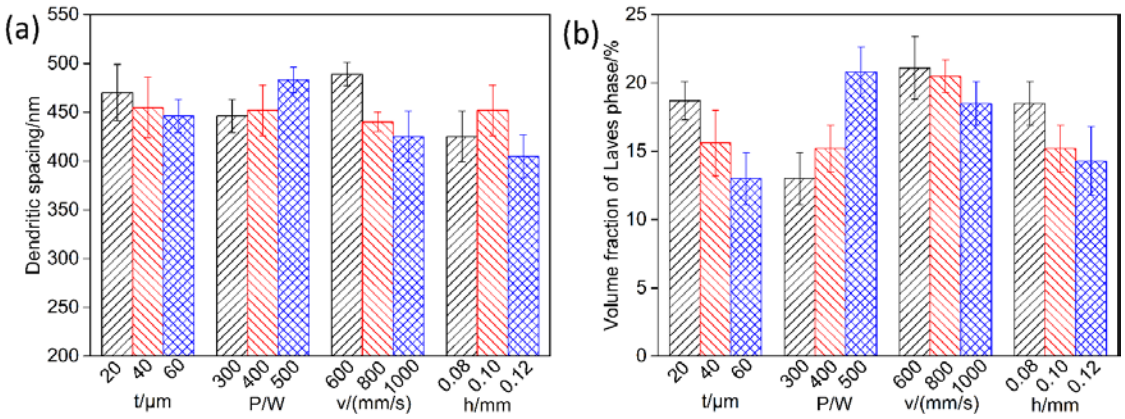

Fig. 3. Statistic results of (a) the average dendrite arm spacing and (b) the volume fraction of Laves phase

Tensile samples were produced using the parameters shown in Table 3 to investigate the effects of process parameters. Results of tensile test are shown in Table 4 and the relationship between mechanical properties and the laser energy density is illustrated in Fig. 4. It can be seen from Fig. 4 that the UTS and YS of different samples do not vary much, while the elongation is volatile and the change law is not apparent.

The precipitation of the γ′ and γ″ phases is the key to improve the strength of IN718. Although the variation of process parameters can change the microstructure and the cooling rate to a certain extent, the precipitation of strengthening phase is still inhibited [10]. The mechanical properties mainly relates to internal defects in such a situation. Therefore, when the relative density is high enough, the mechanical properties are unable to be significantly improved by optimizing the parameters.

Table 4 Mechanical properties of samples fabricated with different process parameters

Sample	YS (MPa)	UTS (MPa)	EL (%)
P1	847 ± 15	1120 ± 11	30.9 ± 0.9
P2	833 ± 19	1127 ± 9	28.9 ± 0.4
P3	832 ± 29	1120 ± 3	23.9 ± 2.5
P4	778 ± 19	1103 ± 14	24.4 ± 2.5
P5	799 ± 13	1098 ± 8	30.2 ± 0.5
P6	773 ± 5	1082 ± 9	34.5± 0.8
P7	815 ± 14	1107 ± 10	28.7 ± 1.2
P8	816 ± 2	1104 ± 7	26.2 ± 1.7
P9	760 ± 3	1069 ± 2	31.3 ± 1.0

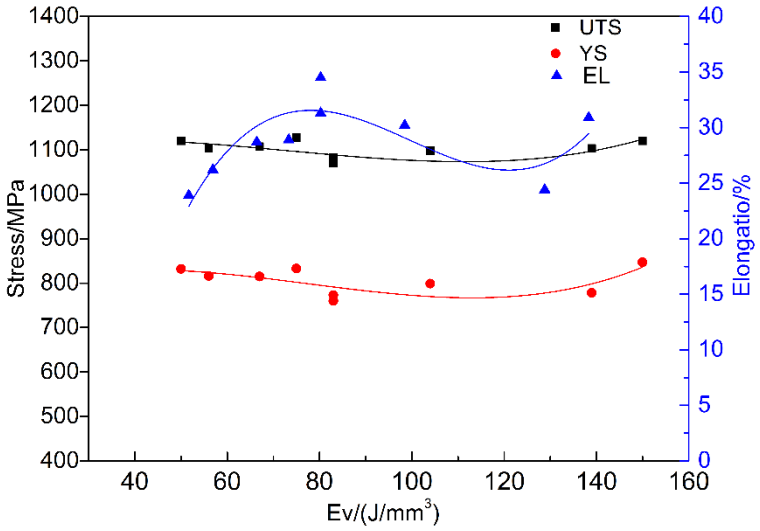

Fig. 4. Mechanical properties of as-fabricated samples in function of the energy density

Effects of heat treatment

Since no distinct difference of tensile properties was found under various parameters, heat treatments were conducted subsequently. Microstructures of the as-fabricated sample solution treated at different temperatures are shown in Fig. 5. When solution treated below 1080 ℃, the dendrites disappear in some regions as shown in Fig. 5a and b, which indicates that partial recrystallization occurs. When solution temperature rises to 1130 ℃, complete recrystallization has taken place and the grains become coarse and equiaxed.

Fig. 6 shows the microstructures of heat-treated samples at high magnification. It can be seen that the microstructures become more homogeneous with temperature increasing. There are still

some residual particles of the Laves phase in the interdendritic regions when solution treated at 980 and 1030 ℃ asshown in Fig. 6a and b, but the Laves phases almost dissolve at higher temperatures.

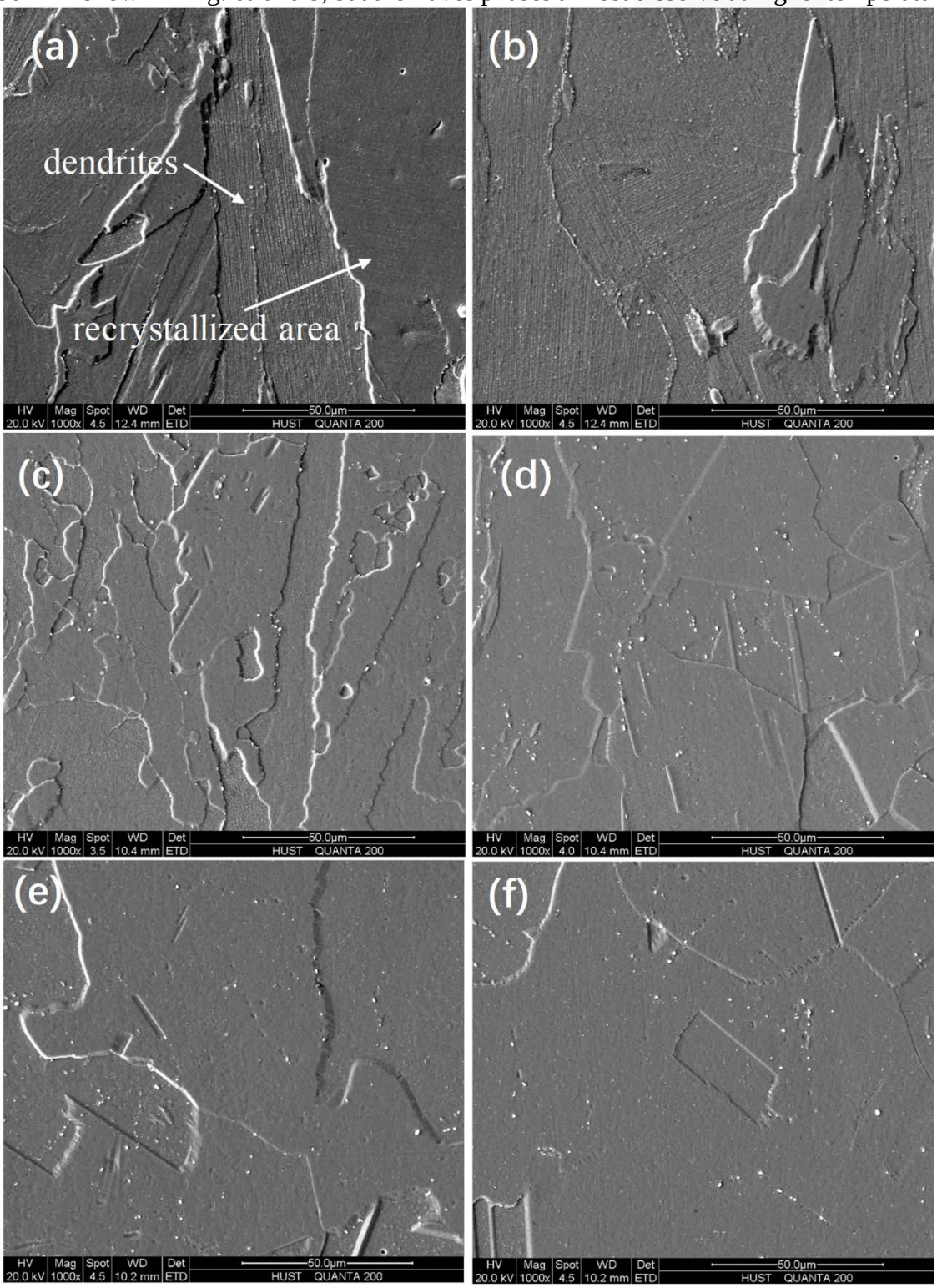

Fig. 5. Microstructure of as-fabricated samples solution treated at different temperatures for 1 h, followed by air cooling. (a) 980 ℃. (b) 1030 ℃. (c) 1080 ℃. (d) 1130 ℃. (e) 1180 ℃. (f) 1230 ℃.

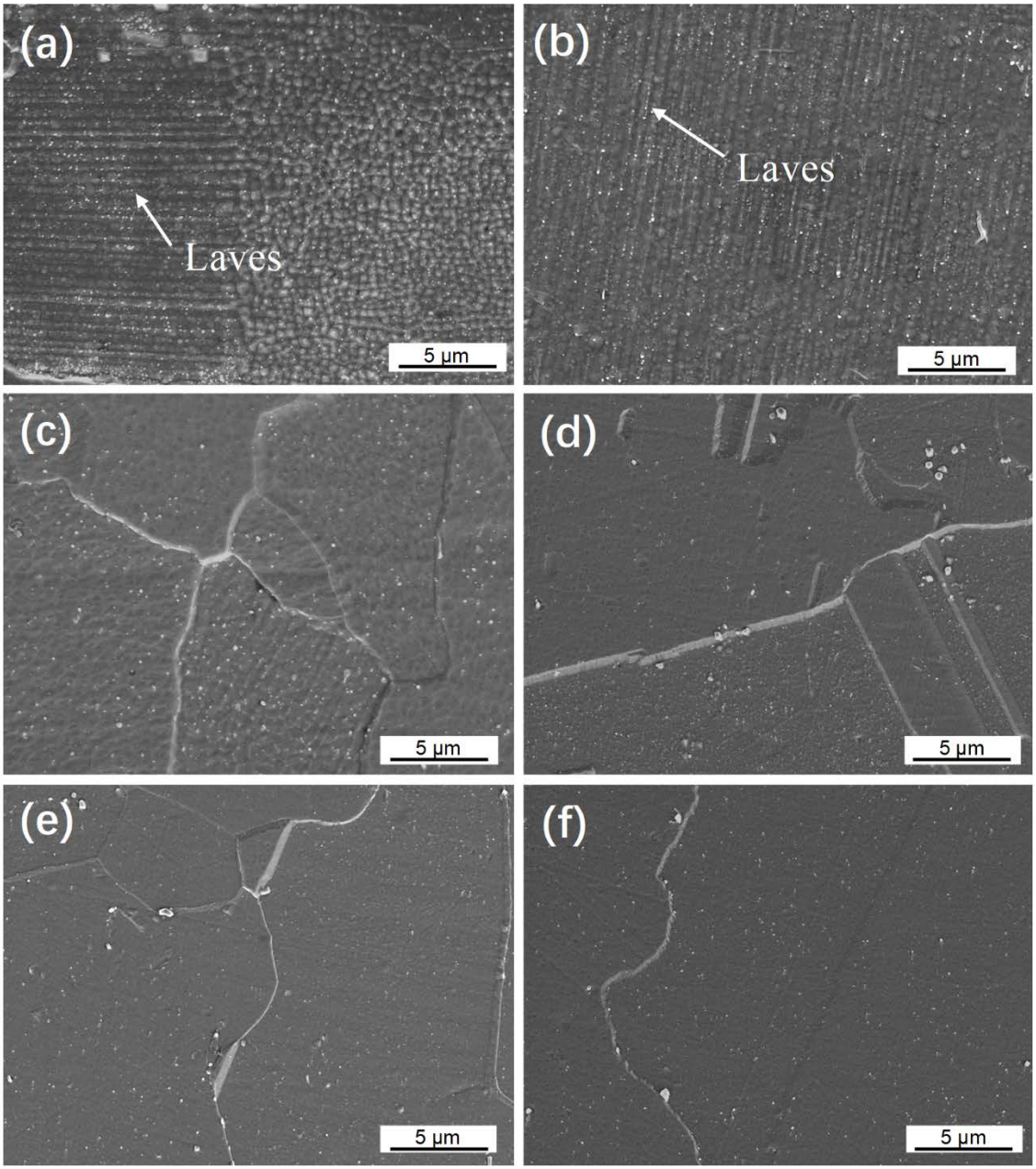

Fig. 6. SEM images of as-fabricated samples solution treated at different temperatures for 1 h, followed by air cooling at high magnification. (a) 980 ℃. (b) 1030 ℃ (c) 1080 ℃ (d) 1130 ℃ (e) 1180 ℃. (f) 1230 ℃

According to the above results, the solution temperature was fixed at 1080 ℃to dissolve Laves phases and obtain fine grains. Aging treatment was carried out following the solution treatment. Tensile properties of heat-treated samples are shown in Table 5 and compared with wrought material [15]. The results show that an obvious increase of the tensile strength occurs with a decrease in the ductility after heat treatment, but the tensile strengths and ductility all exceed the wrought IN718. Therefore, heat treatment is essential to obtain excellent mechanic properties.

Table 5 Mechanical properties of as-fabricated and heat-treated samples

Sample	YS (MPa)	UTS (MPa)	EL (%)
SLM	847 ± 15	1120 ± 11	30.9 ± 0.9
SLM + heat treatment	1369 ± 17	1529 ± 19	18.6 ± 0.9
Wrought	1034	1276	12

Conclusions

In this study, effects of process parameters and heat treatment on microstructure and mechanical properties of selective laser melted Inconel 718 have been studied.

(1) The as-fabricated samples are characterized with fine cellular dendrites with Laves phase precipitating in the interdendritic regions.The average dendrite arm spacing and the volume fraction of Laves phase raise along with the increasing energy input.

(2) When the relative density is high enough, the mechanical properties are unable to be significantly improved by optimizing the parameters.

(3) Laves phase decreases with the solution temperature, while the grain size has the opposite trend. The solution temperature was fixed at 1080 ℃to dissolve Laves phases and obtain fine grains. After solution + aging heat treatment, the tensile strengths and ductility all exceed the wrought Inconel 718.

Acknowledgements

This work is supported by the National Program on Key Basic Research Project of China under Grant no. 613281.

References

[1] N. Nadammal, S. Cabeza, T. Mishurova, T. Thiede, A. Kromm, C. Seyfert, L. Farahbod, C. Haberland, J.A. Schneider, P.D. Portella, Effect of hatch length on the development of microstructure, texture and residual stresses in selective laser melted superalloy Inconel 718, Materials & Design 134 (2017) 139-150.

[2] V. Popovich, E. Borisov, A. Popovich, V.S. Sufiiarov, D. Masaylo, L. Alzina, Functionally graded Inconel 718 processed by additive manufacturing: Crystallographic texture, anisotropy of microstructure and mechanical properties, Materials & Design 114 (2017) 441-449.

[3] X. Li, X. Wang, M. Saunders, A. Suvorova, L. Zhang, Y. Liu, M. Fang, Z. Huang, T.B. Sercombe, A selective laser melting and solution heat treatment refined Al–12Si alloy with a controllable ultrafine eutectic microstructure and 25% tensile ductility, Acta Materialia 95 (2015) 74-82.

[4] T. Trosch, J. Strößner, R. Völkl, U. Glatzel, Microstructure and mechanical properties of selective laser melted Inconel 718 compared to forging and casting, Materials letters 164 (2016) 428-431.

[5] P. Blackwell, The mechanical and microstructural characteristics of laser-deposited IN718, Journal of materials processing technology 170(1-2) (2005) 240-246.

[6] A.F. Rowcliffe, L.K. Mansur, D.T. Hoelzer, R.K. Nanstad, Perspectives on radiation effects in nickel-base alloys for applications in advanced reactors, Journal of Nuclear Materials 392(2) (2009) 341-352.

[7] D.H. Smith, J. Bicknell, L. Jorgensen, B.M. Patterson, N.L. Cordes, I. Tsukrov, M. Knezevic, Microstructure and mechanical behavior of direct metal laser sintered Inconel alloy 718, Materials Characterization 113 (2016) 1-9.
[8] K. Amato, S. Gaytan, L. Murr, E. Martinez, P. Shindo, J. Hernandez, S. Collins, F. Medina, Microstructures and mechanical behavior of Inconel 718 fabricated by selective laser melting, Acta Materialia 60(5) (2012) 2229-2239.
[9] G. Cao, T. Sun, C. Wang, X. Li, M. Liu, Z. Zhang, P. Hu, A. Russell, R. Schneider, D. Gerthsen, Investigations of γ′, γ ″and δ precipitates in heat-treated Inconel 718 alloy fabricated by selective laser melting, Materials Characterization 136 (2018) 398-406.
[10] E. Chlebus, K. Gruber, B. Kuźnicka, J. Kurzac, T. Kurzynowski, Effect of heat treatment on the microstructure and mechanical properties of Inconel 718 processed by selective laser melting, Materials Science and Engineering: A 639 (2015) 647-655.
[11] Q. Jia, D. Gu, Selective laser melting additive manufacturing of Inconel 718 superalloy parts: Densification, microstructure and properties, Journal of Alloys and Compounds 585 (2014) 713-721.
[12] M. Pröbstle, S. Neumeier, J. Hopfenmüller, L. Freund, T. Niendorf, D. Schwarze, M. Göken, Superior creep strength of a nickel-based superalloy produced by selective laser melting, Materials Science and Engineering: A 674 (2016) 299-307.
[13] X. Wang, K. Chou, Effects of thermal cycles on the microstructure evolution of Inconel 718 during selective laser melting process, Additive Manufacturing 18 (2017) 1-14.
[14] Z. Wang, K. Guan, M. Gao, X. Li, X. Chen, X. Zeng, The microstructure and mechanical properties of deposited-IN718 by selective laser melting, Journal of Alloys and Compounds 513 (2012) 518-523.
[15] D. Zhang, W. Niu, X. Cao, Z. Liu, Effect of standard heat treatment on the microstructure and mechanical properties of selective laser melting manufactured Inconel 718 superalloy, Materials Science and Engineering: A 644 (2015) 32-40.
[16] W.M. Tucho, P. Cuvillier, A. Sjolyst-Kverneland, V. Hansen, Microstructure and hardness studies of Inconel 718 manufactured by selective laser melting before and after solution heat treatment, Materials Science and Engineering: A 689 (2017) 220-232.